J Mater Sci: Mater Electron (2021) 32:24964–24970

Structure, thermal stability and dielectric properties of aluminoborosilicate glasses doped with Pr_2O_3

Jingang Zhao[1], Xiaokun Tian[1], Lulu Zhang[1], Ya Qu[1], Chao Wu[1], Fengyang Zhao[2], Xianjing Chen[3], Xunmei Liang[4], Yunlong Yue[1,*], and Junfeng Kang[1,*]

[1] School of Materials Science and Engineering, University of Jinan, Jinan 250000, China
[2] State Key Laboratory for New Technology of Float Glass, 751 Donghai Dadao, Bengbu 233000, China
[3] Shandong Product Quality Inspection Research Institute, 31000 Jingshi East Road, Jinan 250102, China
[4] Shandong Road New Materials Co., Ltd, Taian 271000, China

Received: 1 July 2021
Accepted: 1 September 2021
Published online: 12 September 2021

ABSTRACT

The structure, thermal stability and dielectric properties of aluminoborosilicate glasses with different contents of Pr_2O_3 were researched by XRD, FT-IR, DSC and electronic impedance analyzer. FT-IR results showed that the addition of Pr_2O_3 enhanced the degree of polymerization of glass network. The molar volume decreased at first and then increased, which reached the minimum value with the content of Pr_2O_3 up to 1.5 mol%. With the addition of Pr_2O_3 the glass transition temperature (T_g) showed an upward trend, while Dietzel's thermal stability (ΔT) and the Saad parameter (S) both increased initially to be followed by a decrease, which indicated that the thermal stability of glass can be improved by doping proper content of Pr_2O_3. The dielectric constant (ε_r) and dielectric loss (tanα) both decreased at first then started to go up as the content of Pr_2O_3 increased. When Pr_2O_3 content moved up to 0.5 mol% and 1.5 mol%, the ε_r and tanα reached the minimum values 4.68 and 3.13 $\times$ 10^{-4}, respectively.

1 Introduction

With the rapid progress of digital technology, electronics will develop in the direction of miniaturization and high speed. The printed circuit boards (PCBs) are important parts of electronic products. Glass fiber with low dielectric constant can be used as a reinforcing material in PCB [1, 2]. Many studies show that aluminoborosilicate glass is a suitable material for producing low dielectric glass fiber [3–6]. Electronic glass fiber as a skeleton support material for printing circuit boards can be applied in electronic industry such as aerospace, supercomputers, and communication equipment. The emergence of fifth generation communication system shows that communication is developing in the direction of high frequency and high speed, indicating the dielectric constant and dielectric loss of printed circuit board is

Jingang Zhao and Xiaokun Tian contributed equally to this work and should be considered as cofirst authors

Address correspondence to E-mail: zztg_yueyl@163.com; mse_kangjf@ujn.edu.cn

https://doi.org/10.1007/s10854-021-06954-8

required to be lower. Optimizing dielectric characteristics is of great significance to the development of electronics industry. Therefore, it is necessary to develop glass fibers having superior dielectric properties. Many studies have shown that aluminoborosilicate glass is a complex system [7–9]. Glass former, glass modifier and intermediate (which can be both a glass former and a glass modifier, such as aluminum) are present simultaneously in the aluminoborosilicate glass system. The coordination of aluminum as an intermediate and boron as a former depends on the content of other oxides in the system. The type and content of rare earth oxides also affect the coordination and thus affect the network structure. According to researches, the structure, dielectric properties and thermal stability of glass can be improved by adding rare earth oxides to glass systems [10, 11]. Wang et al. [12, 13] studied the high temperature properties of glass doped with Pr_2O_3, and found that the viscosity of glass at high temperature can be reduced by doping of Pr_2O_3. Johnson et al. [14] studied the influence of Pr_2O_3 and Eu_2O_3 on SiO_2–Na_2O glass structure and found that Pr_2O_3 glasses have higher clustering than the europium glasses. Mekki et al. [15] found a strengthening of the glass structure as Pr^{3+} ions were introduced by magnetisation and X-ray photoelectron spectroscopy. Lakshminarayana et al. [16] found that Pr^{3+} doped borotellurite glass have higher T_g and value of Dietzel's thermal stability (ΔT). Wantana [17] found that the ε values decrease with the increasing concentration of Pr_2O_3.

According to the above researches, some properties of glass can be optimized by doping Pr_2O_3. In this study, the effect of Pr_2O_3 content on the dielectric properties, thermal stability and structure of aluminoborosilicate glasses was investigated systematically.

2 Experimental process

2.1 Sample preparation

As show in Table 1, the compositions of glass samples were listed. The samples were labeled as Pr0 to Pr4 according to the change of Pr_2O_3 content from 0 to 2 mol%. Conventional melting method was used as preparation method in this experiment. The batch materials were mixed with SiO_2 (AR), Al_2O_3 (AR), H_3BO_3(AR), MgO (AR), $CaCO_3$ (AR) and Pr_2O_3 (AR) in an agate mortar for about 30 min. The mixed materials were melted in a Pt–Rh crucible in atmosphere at a temperature range of 1550 °C to 1600 °C for 3 h. The glassy melts were finally poured onto a graphite plate for cooling and molding and instantly annealed at about T_g for 1 h. The obtained glass samples were tested for structure, thermal stability and dielectric properties.

Table 1 Chemical composition of glass samples doped with different content of Pr_2O_3

Sample no	Composition (mol%)					
	SiO_2	Al_2O_3	B_2O_3	CaO	MgO	Pr_2O_3
Pr0	60	10	20	2	7	0
Pr1	60	10	20	2	7	0.5
Pr2	60	10	20	2	7	1.0
Pr3	60	10	20	2	7	1.5
Pr4	60	10	20	2	7	2.0

Deviations from nominal compositions due to the volatilization of boron during the melting process were considered in this experiment. An extra 12% H_3BO_3 was added to reduce the effects of boron volatilization on composition before melting. As shown in Table 2, the practical proportions was measured by chemical quantitative analysis and the volatility of B_2O_3 was be calculated. The calculation results showed that each glass sample had different volatile of B_2O_3. The measured concentrations of B_2O_3 were not far from the nominal values and every ratio of deviation not exceed 3%. So, in the structure analysis the little deviations were ignored.

2.2 Sample characterization

In this experience, the amorphous structure of samples powder were proved by X-ray diffractometer (D8 ADVANCE).

The FTIR experiment used potassium bromide (KBr) pellet method and Nicolet-380 infrared spectrophotometer. The FTIR of glass samples obtained in the frequency range of 400–2000 cm^{-1}.

Archimedes method was used to measure the density (ρ) at 25 °C. The immersion fluid was distilled water. The relative error was ± 0.001 g/cm^3. The calculated formula of molar volume (V_M) was (1) [18]:

Table 2 The quality content of B_2O_3 in all glasses (wt%)

Sample no	Pr0	Pr1	Pr2	Pr3	Pr4
Nominal ratio (%)	24.3	23.7	23.2	22.6	22.1
Proportion before melting (%)	27.2	26.5	26.0	25.3	24.8
Measured proportion after melting (%)	24.9	24.3	23.8	23.1	22.6
Volatility (%)	8.51	8.45	8.41	8.74	8.69

All data are calculated only for oxides

$$V_M = M/\rho \quad (1)$$

where ρ is the measured density of the glass and M is the molar mass.

The calculated formula of theoretical density (ρ_{cal}) was (2) [18].

$$\rho_{cal} = \sum \rho_i x_i \quad (2)$$

where ρ_i is density of each component i, x_i is the molar fraction of each component i.

The DSC analysis of samples was obtained by TGA/DSC1/1600HT synchronous thermal analyzer. The DSC measurements were carried out in atmosphere within 20 °C–1400 °C and the heating rate was 10 °C/min. The glass transition temperature (T_g), the crystallization onset temperature (T_c) and the crystallization peak temperature (T_p) can be obtained. Then ΔT and S were calculated by formulas follows (4) and (5) [19]

$$\Delta T = (T_c - T_g) \quad (4)$$

$$S = \frac{(T_p - T_c)\Delta T}{T_g} \quad (5)$$

The dielectric properties of glass were measured in air at 25 °C. This measurement used Agilent 4292A Impedance Analyzer at 1 MHz. Test fixture was Agilent 16451B. The tested samples were processed into the dimensions of 10 mm × 10 mm × 2 mm. And the surfaces of the samples were polished thoroughly.

3 Result analysis

3.1 XRD

The XRD patterns of all glass samples are showing Fig. 1. A broad diffuse scattering occurs at different angles. It proves that all glass samples are amorphous [20].

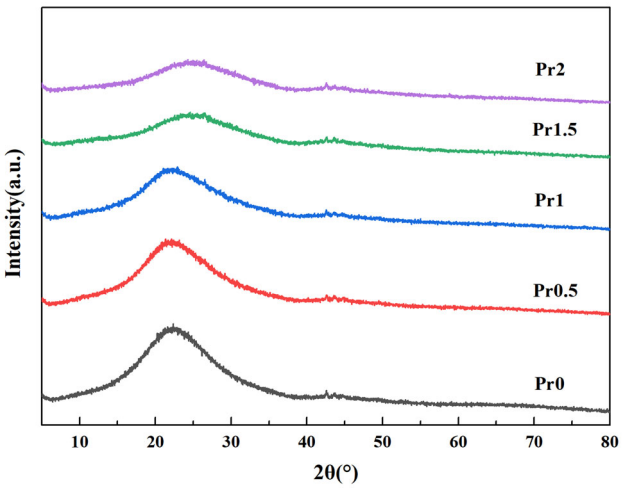

Fig. 1 The X-ray diffraction pattern of Pr0, Pr1, Pr2, Pr3 and Pr4

3.2 FTIR spectra

The Infrared Spectroscopic of glass samples are shown in Fig. 2. The FTIR spectra have six main characteristic absorption peaks at about 462, 685, 795, 923, 1090 and 1400 cm^{-1}, respectively. The band observed at about 400 cm^{-1}–480 cm^{-1} corresponds to the bending vibration of Si–O–Si bond and the asymmetric bending vibration of Si–O–Al band [20]. The band at about 600 cm^{-1}–740 cm^{-1} results in the stretching vibration of Al–O–Al between [AlO_4]. [21] The intensity of the absorption band is increased, which indicating that the content of [AlO_4] is increased as the content of Pr_2O_3 increases. Research shows that the addition of Pr_2O_3 can provide free oxygen, which transforms [AlO_5] and [AlO_6] into [AlO_4] then reduces the amount of non-bridge oxygen [22]. The band at about 760 cm^{-1}–825 $cm^{-1}$is due to the Si–O–Al stretching vibration between [SiO_4] and [AlO_4] [23, 24]. The band observed at about 923 cm^{-1} corresponds to the stretching vibration of B–O–B bond [25, 26], and its strength increases with the addition of Pr_2O_3. The characteristic band at 1400 cm^{-1} derives from the B–O band in the [BO_3]

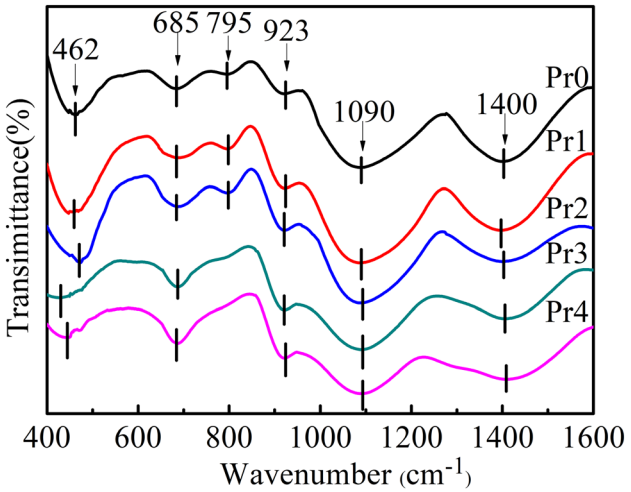

Fig. 2 FTIR spectrum of glass samples Pr0, Pr1, Pr2, Pr3 and Pr4

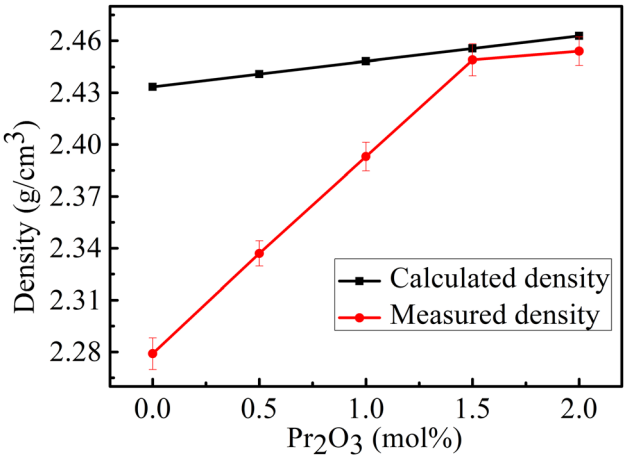

Fig. 3 The change of density of glass samples Pr0, Pr1, Pr2, Pr3 and Pr4

triangles [27], and its strength decreases with the addition of Pr_2O_3. These two changes indicate that the addition of Pr_2O_3 can transform $[BO_3]$ to $[BO_4]$. Research shows that the Pr^{3+} also can compensate for the excess negative charge of $[BO_4]$ and $[AlO_4]$ [28]. The band at about 1090 cm^{-1} represents the T–O stretching vibration of $[TO_4]$ (T = Si and Al) tetrahedron structural units [29], and its vibrational absorption peak moves towards the high wave number. It indicates that concentration of $[TO_4]$ is increased. The reason for this increase is that addition of Pr_2O_3 changes the Al^{3+} from glass modifier to the glass former and Mg^{2+} and $Ca^{2+}$from glass modifier to charge compensation role [30]. Through the above analysis, it is proved distinctly that doping Pr_2O_3 improved the degree of polymerization of glass structure.

3.3 Density and molar volume

Density is a basic macroscopic parameter that characterizes the structure of glass. The density is mainly determined by the relative atomic mass of the glass component and the type of glass structural groups.

Figure 3 and Table 3 show that with addition of Pr_2O_3 the measured density of glass increases from 2.279 to 2.454 g/cm^3, and its variation trend is consistent with the calculated density. This increase is mainly due to the relative atomic mass of Pr which is more massive than other atomic [31]. In addition, the change of glass network structure resulting from different Pr_2O_3 content also has complex influence on the density. With the addition of a small amount of Pr_2O_3, the degree of network polymerization is increased and the Pr^{3+} can fill in the gaps in the glass network, which causes the density of the glass to increase.

In this experiment, with the addition of Pr_2O_3 the molar volume decreases at first and then increases in Table 3. When 1.5 mol% of Pr_2O_3 is added, the molar volume reaches the minimum value, indicating that as this content of the Pr_2O_3 the glass sample has the densest glass network structure. There are two major factors effecting the change of molar volume. One is positive effect of increased degree of polymerization on glass structure. FTIR spectra result indicates that the degree of network polymerization is increased with the doping of Pr_2O_3. The other is a negative effect of destruction of Pr^{3+} on glass structure due to its oversize ion radius [32], and this effect is intensified with addition of Pr_2O_3. When content of the $Pr_2O_3 < 1.5$ mol%, the positive effect is greater than the negative one, which results the decrease of molar volume. When content of the $Pr_2O_3 > 1.5$ mol%, the negative effect is greater than the positive one, which results the increase of molar volume.

3.4 Thermal stability studies

The DSC curves of glass samples are shown in Fig. 4. There are three characteristic temperatures of glass samples in the thermal analysis curves. They are the glass transition temperature (T_g), the crystallization onset temperature (T_c) and the crystallization peak temperature (T_p) [33]. T_g is an important thermal parameter of glass, which is depend on the

Table 3 Parameters: measured density (ρ), calculated density (ρ_{cal}), molar volume (V_m)

Sample no	ρ(g/cm^3)(25 °C)	ρ_{cal}(g/cm^3)	V_m(cm^3/mol)
Pr0	2.279	2.433	28.419
Pr1	2.337	2.441	28.284
Pr2	2.393	2.448	28.174
Pr3	2.449	2.456	28.063
Pr4	2.454	2.463	28.533

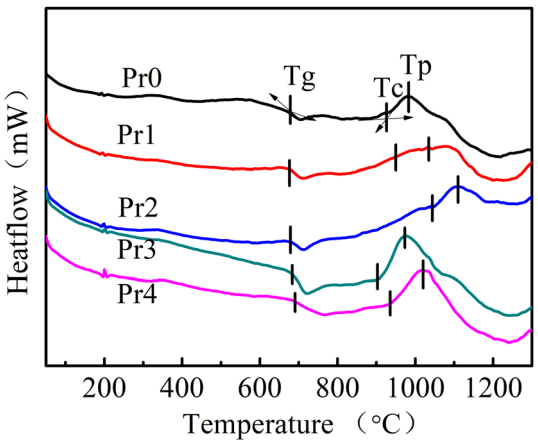

Fig. 4 Thermal analysis curves of glass samples Pr0, Pr1, Pr2, Pr3 and Pr4

connectivity of glass network structure and cation field strength. With the addition of Pr_2O_3, the change of T_g shows an upward trend in Fig. 3. One reason for this change is that the Pr^{3+} has the greater aggregation capacity due to larger cation field intensity, which increases the stability of the glass [34]. Another reason is that the addition of Pr_2O_3 improves the degree of polymerization of glass structure, which is proved in above experimental results of infrared spectrum. The changes of T_c and T_p are irregular. The reason for it is that there is a complex microstructure due to the interaction and competition of the glass formers including SiO_2, Al_2O_3 and B_2O_3 with the addition of Pr_2O_3. [35–37] But Dietzel's thermal stability (ΔT) and Saad-Poulin's thermal stability parameter (S) are commonly used to indicate the thermal stability of glass samples in researches [19].

The value of S and ΔT can indicate the ability of glass to resist crystallization after the glass is formed [38]. The larger value of S and ΔT indicates the

Table 4 Characteristic temperatures of glass samples

Serial number	T_g (°C)	T_c (°C)	T_p (°C)	ΔT (°C)	S (°C)
Pr0	678	926	982	248	20.48
Pr1	676	949	1034	273	34.33
Pr2	678	1043	1109	365	35.53
Pr3	683	902	972	219	22.45
Pr4	690	935	1020	245	30.18

aluminoborosilicate glass will be more stable in the form of glass. As show in Table 4, the characteristic temperature parameters S and ΔT both increase firstly and then decrease. When 1.0 mol% of Pr_2O_3 is added, S and ΔT reach the maximum value 365 °C and 35.53 °C, respectively. It indicates that the aluminoborosilicate glass in this experiment can achieve superior thermal stability by doping Pr_2O_3. When content of Pr_2O_3 exceeds 1.0 mol%, ΔT and S are decreased, indicating that thermal stability is decreased. The reason for this deterioration may be that doping too much Pr_2O_3 causes partial crystallization or phase separation occurs in the glass at temperature above T_g [39].

3.5 Dielectric properties

Figure 5 shows the effects of different contents of Pr_2O_3 on dielectric properties of glasses. The dielectric constant is mainly affected by the polarization of ions, electrons and space charges [40, 41]. In this experiment, with the addition of Pr_2O_3 dielectric constant decreases initially, followed by an increase, and reaches a minimum value when 0.5 mol% Pr_2O_3 is added. The change of the dielectric constant depends on two main factors: the network structure of glass and the magnitude of the ionic polarizability. The decrease of dielectric constant is mainly result of tighter network structure due to a small amount addition of Pr_2O_3. With the addition of Pr_2O_3 the main effect on increase of dielectric constant is increased total ionic polarizability of glass due to Pr^{3+} has greater cationic polarization than other components [42, 43]. When the content of Pr_2O_3 exceeds 0.5 mol%, the effect of cationic polarization is greater than that of denser glass network, which causes the dielectric constant increases. And when content of Pr_2O_3 exceeds 1.5 mol%, the structure of glass starts be loose, which has an effect on the increase of dielectric constant like the effect of greater

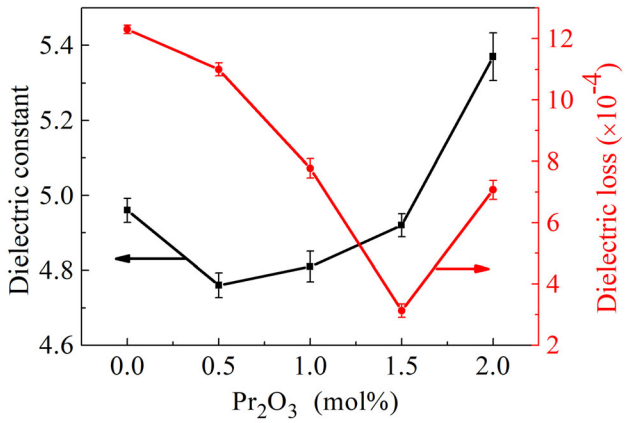

Fig. 5 Dielectric properties of samples Pr0, Pr1, Pr2, Pr3 and Pr4

cationic polarization of Pr^{3+}. So, the dielectric constant is greatly increased with content of Pr_2O_3 > 1.5 mol%. As the content of Pr_2O_3 increasing, dielectric loss starts with a downward trend and then increases, and reaches a minimum value when 1.5 mol% Pr_2O_3 is added. The dielectric loss is mainly affected by the ability of ion migration [44]. The reduction of dielectric loss is due to that the addition of a small amount Pr_2O_3 promote the glass network structure be more compact. The compact network structure hinders cation movement and space charge polarization. Moreover, Pr^{3+} can get in the gap of network to connect the anion group for compensating the negative charge, which reduces space charge polarization of inhomogeneous dielectric. Thereby dielectric loss is decreased by doping a small quantity of Pr_2O_3. The dielectric loss is increased when the content of Pr_2O_3 exceeds 1.5 mol%. When 1.5 mol% Pr_2O_3 is added, glass network can be damaged and be looser. The loose structures increased cation motion and space charge polarization, thereby increasing dielectric loss [45].

4 Conclusions

In this work, the effect of Pr_2O_3 on the structure, thermal stability and dielectric properties of the aluminoborosilicate glasses were investigated. FTIR results show that doping Pr_2O_3 transforms [AlO_5], [AlO_6] to [AlO_4] and [BO_3] to [BO_4], which enhances the degree of glass network polymerization. Analysis about density and molar volume show that doping a moderate amount of Pr_2O_3 can improve the compactness of the glass structure but excessive Pr_2O_3 can destroy the compact structure of the glass. Thermal stability studies show that with the addition of Pr_2O_3, ΔT and S increase initially, follow by a decrease, and both reach a maximum value (365 °C and 35.53 °C) when 1.0 mol % Pr_2O_3 is added. It indicates that proper addition of Pr_2O_3 can optimize the thermal stability of aluminoborosilicate glass. Dielectric properties studies show that as the addition of Pr_2O_3, the dielectric constant and dielectric loss increase firstly and decrease later. When 0.5 mol% Pr_2O_3 was added, the dielectric constant reaches the minimum (4.68). When 1.5 mol% Pr_2O_3 was added, the dielectric loss reaches the minimum (3.13×10^{-4}). It is observed that the dielectric properties of glass can be improved by addition of moderate Pr_2O_3.

Acknowledgements

This paper was funded by National Natural Science Foundation of China (Nos. 51872117, 51804131, 52072148 and 51672105), Natural Science Foundation of Shandong Province (No. ZR2019BEM002), and Opening Project of State Key Laboratory of Advanced Technology for Float Glass (No. 2020KF01)

References

1. A. Sridhar, D.J.V. Dijk, R. Akkerman, Thin Solid Films **517**(16), 4633–4637 (2009)
2. S.X. Huang, S. Li, F.N. Wu, Y.L. Yue, J. Inorg. Organomet. Polym. Mater. **25**, 816–822 (2015)
3. I.J. Choi, Y.S. Cho, J. Electroceram. **23**, 185 (2009)
4. X.H. Zhang, Y.L. Yue, H.T. Wu, J. Mater. Sci. Mater. Electron. **24**, 2755–2760 (2013)
5. H. Darwish, M.M. Gomaa, J. Mater. Sci. Mater. Electron. **17**, 35–42 (2006)
6. Y.L. Yue, X.H. Zhang, Y.C. Xu, S.X. Huang, P.P. Chen, Mater. Lett. **136**, 356–358 (2014)
7. T.A. Taha, S. Alomairy, S.A. Saad, H.O. Tekin, M.S.A. Buriahif, Ceram. Int. **47**(14), 20201–20209 (2021)
8. Lu. Deng, Du. Jincheng, J. Non-Cryst. Solids **453**, 177–194 (2016)
9. J. Wu, J.F. Stebbins, J. Non-Cryst. Solids **356**(41–42), 2097–2108 (2010)
10. X.H. Zhang, Y.L. Yue, H.T. Wu, Surf. Rev. Lett. **19**(6), 1250062 (2012)

11. H.T. Liu, S. Li, F.N. Wu, Z.Y. Chang, S.X. Huang, Y.L. Yue, J. Mater. Sci. Mater. Electron. **27**, 9821–9827 (2016)
12. M.T. Wang, J.S. Cheng, Q.M. Liu, P.J. Tian, M. Li, J. Nucl. Mater. **400**(2), 107–111 (2010)
13. M.T. Wang, J.S. Cheng, M. Li, J. Rare Earth. **28**(S1), 308–311 (2010)
14. J.A. Johnson, C.J. Benmore, D. Holland, J. Du, B. Beuneu, A. Mekki, J. Phys. Condens. Mater. **23**(6), 065404 (2011)
15. A. Mekki, K.A. Ziq, D. Holland, C.F. Mcconville, J. Magn. Magn. Mater. **260**(1–2), 60–69 (2003)
16. G. Lakshminarayana, S.O. Baki, A. Lira, I.V. Kityk, M.A. Mahdi, J. Non-Cryst. Solids **459**, 150–159 (2017)
17. N. Wantana, E. Kaewnuam, Y. Ruangtaweep, D. Valiev, S. Stepanov, K. Yamanoi, H.J. Kim, S. Kothan, J. Kaewkhao, J. Non-Cryst. Solids **554**, 120603 (2021)
18. O.A. Zamyatin, A.D. Plekhovich, E.V. Zamyatina, A.A. Sibirkin, J. Non-Cryst, Solids **452**, 130–135 (2016)
19. M.G. Drexhage, C.T. Moynihan, M. Robinson, Mater. Sci. Forum **19–20**, 11–18 (1987)
20. L. Hwa, S. Hwang, L. Liu, J. Non-Cryst. Solids **238**(3), 193–197 (1998)
21. H. Darwish, M.M. Gomaa, J. Mater. Sci. Mater. El. **17**, 35–42 (2006)
22. L.L. Zhang, Y. Qu, X.G. Wan, J.L. Zhao, J.G. Zhao, Y.L. Yue, J.F. Kang, J Non-Cryst. Solids **532**, 119886 (2020)
23. J.P. Hamilton, S.L. Brantley, C.G. Pantano, L.J. Criscenti, J.D. Kubicki, Geochim. Cosmochim. Acta **65**(21), 3683–3702 (2001)
24. L. Stoch, M. Środa, J. Mol. Struct. **511–512**, 77–84 (1999)
25. H. Darwish, M.M. Gomaa, J. Mater. Sci. Mater. El. **17**(1), 35–42 (2006)
26. E.I. Kamitsos, M.A. Karakassides, G.D. Chryssikos, J. Phys. Chem. **91**(5), 1073–1079 (1987)
27. L.L. Zhang, Y.D. Lu, J.F. Kang, Q.S. Shi, Y.L. Wang, Y. Qu, Y.L. Yue, J. Mater. Sci.-Mater. El. **29**(7), 5746–5752 (2018)
28. M. Rozanski, K. Wisniewski, J. Szatkowski, C. Koepke, M. Środa, Opt. Mater. **31**(3), 548–553 (2009)
29. W.-F. Du, K. Kuraoka, T. Akai, T. Yazawa, J. Mater. Sci. **35**(19), 4865–4871 (2000)
30. M.T. Wang, F. Long, M. Li, J.S. Cheng, F. He, W. Deng, R. Dongolc, Mater. Chem. Phys. **179**, 304–309 (2016)
31. L. Pauling, J. Am. Chem. Soc. **49**(3), 765–790 (1927)
32. O.A. Zamyatin, A.D. Plekhovich, E.V. Zamyatina, A.A. Sibirkinab, J. Non-Cryst. Solids **452**, 130–135 (2016)
33. M.K. Mahapatra, K. Lu, R.J. Bodnar, Appl. Phys. A **95**, 493–500 (2009)
34. F. Lofaj, R. Satet, J.M. Hoffmann, A.R. de Arellano Lópezb, J. Eur. Ceram. Soc. **24**(12), 3377–3385 (2004)
35. L.S. Du, J.F. Stebbins, J. Non-Cryst. Solids **351**(43–45), 3508–3520 (2005)
36. G. Tricot, Phys. Chem. Chem. Phys. **18**(38), 26764–26770 (2016)
37. L. Deng, J.C. Du, J. Non-Cryst. Solids **453**, 177–194 (2016)
38. M. Monisha, M.S. Murari, M.I. Sayyed, H. Al-Ghamdi, A.H. Almuqrin, G. Lakshminarayana, S.D. Kamath, Mater. Chem. Phys. **270**, 124787 (2021)
39. Y. Zhang, C.H. Lu, Y.R. Ni, Z.Z. Xu, J. Chin. Rare Earth Soc. **25**(5), 578–583 (2007)
40. Z.A. Alrowaili, T.A. Taha, M.I. Brahim, K.M.A. Saron, J. Electron. Mater. **50**, 1102–1109 (2021)
41. Z.A. Alrowaili, T.A. Taha, M. Ibrahim, K.M.A. Saron, Eur. Phys. J. Plus. **136**, 567 (2021)
42. T.A. Taha, A. Hassona, S. Elrabaie, M.T. Attia, Appl. Phys. A **126**, 761 (2020)
43. T.A. Taha, S.A. Saad, Mater. Chem. Phys. **255**, 123574 (2020)
44. P.R. Prezas, M.J. Soares, F.N.A. Freire, M.P.F. Graçaa, Mater. Res. Bull **68**, 314–319 (2015)
45. V. Dimitrov, T. Komatsu, J. Solid State Chem. **163**(1), 100–112 (2002)